# WAVELET-BASED ESTIMATION OF HEMODYNAMIC RESPONSE FUNCTION FROM fMRI DATA

R. SRIKANTH

*Department of Electrical Engineering, Indian Institute of Science,*
*Bangalore, Karnataka 560012, India*
*srikanth@ee.iisc.ernet.in*

A. G. RAMAKRISHNAN

*Department of Electrical Engineering, Indian Institute of Science,*
*Bangalore, Karnataka 560012, India*
*ramkiag@ee.iisc.ernet.in*

We present a new algorithm to estimate hemodynamic response function (HRF) and drift components of fMRI data in wavelet domain. The HRF is modeled by both parametric and nonparametric models. The functional Magnetic resonance Image (fMRI) noise is modeled as a fractional brownian motion (fBm). The HRF parameters are estimated in wavelet domain by exploiting the property that wavelet transforms with a sufficient number of vanishing moments decorrelates a fBm process. Using this property, the noise covariance matrix in wavelet domain can be assumed to be diagonal whose entries are estimated using the sample variance estimator at each scale. We study the influence of the sampling rate of fMRI time series and shape assumption of HRF on the estimation performance. Results are presented by adding synthetic HRFs on simulated and null fMRI data. We also compare these methods with an existing method,[1] where correlated fMRI noise is modeled by a second order polynomial functions.

*Keywords*: Bayesian estimation; wavelets; fMRI; HRF modeling; $1/f$ noise.

## 1. Introduction

Functional Magnetic Resonance Imaging (fMRI) is a non-invasive imaging technique that can be used to study the function of brain. fMRI measures changes in blood oxygenation and blood volume that result from neural activity. This Blood Oxygen Level Dependent (BOLD) response gives a contrast which distinguishes between activated and non-activated regions of the brain for a given task.

A typical fMRI experiment consists of periodic blocks of baseline and activation. During the baseline, the subject is at rest or at baseline condition and during the activation period, the subject performs a specified cognitive task. fMRI images are continuously acquired during both periods. One baseline followed by activation and then followed by baseline is termed as a cycle. One common way of modeling the fMRI time-series is by a convolution model[2]: The observed time-series at each voxel is the output of a linear filter with the boxcar function, representing the design paradigm, as the input. The impulse response of the filter is called as Hemodynamic Response Function (HRF).

Significant work has been done so far,[3,4] in identifying the activated regions for a given task. With the increase in time resolution of fMRI data, there is a significant interest in estimating the temporal characteristics of fMRI data.[5] Estimation of HRF is important in not only identifying the regions of activation but also in finding the relative time of activation of different brain regions. This can be achieved by determining the delay time of HRF at various brain regions. Amplitudes of the response at different

locations give the strength of response at these locations for a given task. Estimation of HRF also helps in event-related design paradigms[5] where HRFs will be different for events and the task. Several parametric models like gamma,[2] poisson and gaussian functions[5] have been used to model HRF.

BOLD signal in fMRI time-series is corrupted by physiological noise due to cardiac and respiratory cycles and their aliased versions, thermal and scanner noise. Physiological noise components appear as trends or fluctuations in the voxel time-series. It is observed that fMRI time-series under null conditions exhibit long term dependence (or $1/f$ property) which can be modeled by fractional Brownian motion (fBm).[3] In this work, We model HRF by both parametric (Gaussian function) and nonparametric models and the noise is modeled by fBm. We study the influence of sampling time (TR) and shape assumption on the estimation performance. We also compare our method with the method of Ref. 1, where correlated fMRI noise is modeled by a second order polynomial functions. Results are presented by adding synthetic HRFs on simulated and null fMRI data.

## 2. Fractional Brownian Motion

fMRI voxel time-series exhibits serial dependence even in the absence of experimental effects. This colored fMRI noise typically has disproportionate spectral power at low frequencies, i.e., its spectrum has $1/f$-like behavior. Physical systems in which many particles are relaxing from excited states at different rates are well known generators of $1/f$-like noise. The coloring in fMRI noise in the absence of physiological causes can be attributed to physical effects.[6] Fractional Brownian motion (fBm) is a good tool to model these processes. Below, we give a brief review of fBm processes and the details can be obtained from Refs. 7 and 8.

A fBm $B(t)$ is a zero mean, non stationary, and non-differentiable function of time. The mean square difference between values of the function at any two time points is proportional to the time difference $\Delta$ raised to the power of twice the Hurst exponent, $H$. For fBm processes, H has value between 0 and 1; i.e.,

$$E(B(t) - B(t - \Delta)^2) \approx |\Delta|^{2H} \tag{1}$$

If $\Delta = 0$, the variance of the process is non stationary

$$E(B^2(t)) \approx t^{2H} \tag{2}$$

The covariance between the process at two times $t$ and $u$ is given by,

$$E(B(t), B(u)) = 0.5\sigma^2(|t|^{2H} + |u|^{2H} - |t - u|^{2H})$$
$$0.5\sigma^2 = \Gamma(1 - 2H)cos(\pi H)/\pi H \tag{3}$$

From the Eq. (3), it can be shown that $B(t)$ is self-affine, i.e., rescaling the process in time by an arbitrary scalar $s > 0$ yields a process $B(st)$ with statistical properties identical to those of the process $s^H B(t)$ generated by rescaling its values on the original time scale by the scalar $s^H$. From this self-affine property, it follows that the fractional dimension $D$ of the process is simply related to its Hurst component by

$$D = T + 1 - H \tag{4}$$

where $T$ is the topological dimension of the data. For a time-series, $T = 1$; therefore $D = 2 - H$. Ordinary Brownian motion is the special case of fBm occurring when $H = 0.5$.

In Refs. 9 and 10, it was shown that wavelet transform with a sufficient number of vanishing moments decorrelates a fBm process. This means that the wavelet coefficients across and within scales are uncorrelated or weakly correlated even if the signal is correlated in the time domain. It was further shown in Refs. 7 and 11 that wavelet decomposition also possesses optimally decorrelating or Karhunen-Loeve properties for the wider class of $1/f$-like signals. For fBm processes, the expected correlation between any two wavelet coefficients $w_{j,k}$ and $w_{j',k'}$ is (first index refers to scale and the second to time)

$$E(w_{j,k}, w_{j',k'}) \propto O(|2^j k - 2^{j'} k'|^{2(H-R)}) \tag{5}$$

Thus, the expected correlation between any two wavelet coefficients at the same scale $w_{j,k}$ and $w_{j,k'}$ is

$$E(w_{j,k}, w_{j',k'}) \propto O(|k - k'|^{2(H-R)}) \tag{6}$$

where $R$ is the number of vanishing moments of the mother wavelet. These results imply that the second order stochastic properties of wavelet coefficients are stationary within and across the scales, even if the original time-series is non stationary. Since the Hurst component $H < 1$ and if $R \geq 2$, the

correlation between any two pairs of wavelet coefficients decays rapidly as inverse square of their separation within and across scales. More precisely, it is shown in Ref. 12 that provided $R > 2H + 1$, the inter coefficient correlations decay hyperbolically fast within levels and exponentially fast between levels. This suggests that the minimum number of vanishing moments required to decorrelate fBm process with $0 < H < 1$ is 4. Wavelet filters with a large number of vanishing moments have long filter lengths. Since fMRI time-series typically have short lengths, boundary correction results in artefactual inter coefficient correlations. For this reason, we use fourth-order daubechies wavelet, which is the most compactly supported wavelet with four vanishing moments.

We use the decorrelating property of wavelet transforms to build a probability model for fMRI time-series. This model, in turn, is used to estimate the hemodynamic response function in the wavelet domain.

## 3. Probability Model for fMRI Time-Series

BOLD response of the brain for a given task can be modeled as the convolution of the HR function and the input task.[2] The input task $x(t)$ is considered as a binary function of time which has a value of '1' during the task and a '0' during the rest period.

$$y_m(t) = \sum_{k=1}^{K} x(t-k)h_m(k) + \beta_m(t) + e_m(t),$$
$$t = (K+1) \cdots N \quad (7)$$

where, $y_m(t)$ is the observed $m$th voxel time-series, $h_m(t)$ is the system impulse response, $\beta_m(t)$ is the trend, $e_m(t)$ is the additive noise component and $K$ is the length of the system response. We model the system response $\mathbf{h_m}$ by both Gaussian function and smooth FIR filters. For convenience, we omit the subscript "m" denoting HRF for each voxel time-series. Note that HRF is computed separately at each voxel. Also, the noise components $e(t)$ and $\beta(t)$ are modeled separately for each voxel time-series. The above equation can be written in matrix form as:

$$\mathbf{y} = \mathbf{Xh} + \beta + \mathbf{e} \quad (8)$$

where $\mathbf{X}$ is a $(N - K \times K)$ convolution matrix and $\mathbf{y}$, $\beta$, $\mathbf{e}$ are $(N - K \times 1)$ vectors. We model the noise

component $\mathbf{e}$ as a fBm process. Therefore, the probability of $\mathbf{y}$ given $\mathbf{h}$ is

$$p(\mathbf{y}|\mathbf{h}) \sim N(\mathbf{Xh} + \beta, \mathbf{C}) \quad (9)$$

where $\mathbf{C}$ is the covariance matrix whose elements are given by (3). Multiplying WT matrix $\mathbf{W}_T$ (or applying discrete wavelet transform) on both sides of (8), we have

$$\mathbf{W}_T\mathbf{y} = \mathbf{W}_T\mathbf{Xh} + \mathbf{W}_T\beta + \mathbf{W}_T\mathbf{e} \quad (10)$$

where, $\mathbf{W}_T\mathbf{y}$, $\mathbf{W}_T\beta$ and $\mathbf{W}_T\mathbf{e}$ are, respectively, the wavelet coefficients of the observed signal, drift and noise. Let $\mathbf{y}_w = \mathbf{W}_T\mathbf{y}$, $\mathbf{X}_w = \mathbf{W}_T\mathbf{X}$, $\beta_w = \mathbf{W}_T\beta$ and $\mathbf{e}_w = \mathbf{W}_T\mathbf{e}$. Then the above equation can be written compactly as:

$$\mathbf{y}_w = \mathbf{X}_w\mathbf{h} + \beta_w + \mathbf{e}_w \quad (11)$$

For example, for J scales ($J = log_2 N$, where N is length of the vector), $\mathbf{y}_w$ is

$$\mathbf{y}_w = \big[ ay_1^J, dy_1^J, dy_1^{J-1}, \ldots, dy_{2^{-J}N}^{J-1},$$
$$\ldots, dy_1^1, \ldots, dy_{2^{-1}N}^1 \big]^t \quad (12)$$

where, $ay_k^j$ and $dy_k^j$ (subscript $k$ denotes time index and superscript $j$ indicates scale) are approximate and detail coefficients, respectively. The columns of $\mathbf{X}_w$ can be obtained by applying wavelet transform to each column of $\mathbf{X}$. Therefore, the probability model for $\mathbf{y}_w$ given $\mathbf{h}$ is

$$p(\mathbf{y}_w|\mathbf{h}) \sim N(\mathbf{X}_w\mathbf{h} + \beta_w, \Lambda) \quad (13)$$

where, $\Lambda$ is a diagonal matrix assuming that WT decorrelates the noise process $\mathbf{w}$. The diagonal elements of $\Lambda$ are variances of wavelet coefficients at each scale.

$$\Lambda = diag\big[ \sigma_J^2, \sigma_J^2, \sigma_{J-1}^2, \ldots, \sigma_1^2 \big] \quad (14)$$

## 4. Estimation of HRF and Drift

### 4.1. Gaussian model for HRF

Hemodynamic response refers to the local change in blood oxygenation as an effect of increased neuronal activity. This response can be modeled as an output of a linear filter for an input of unit impulse. In this section, we model the system response (HRF) by a

Gaussian function, where the parameters give a physiological interpretation.[5] The HRF is represented as:

$$h(t) = \eta \exp(-(t.TR - \mu)^2/\sigma^2) \qquad (15)$$

where, $\mu$ is the time lag from the onset of the stimuli to the peak of HR; $\sigma$ reflects the rise and decay time and $\eta$ is the amplitude of the response and $TR$ is the sampling period. Let $\theta = [\mu, \sigma, \eta]$ denote the unknown parameters of the HRF.

Now, the estimation of HRF boils down to estimating the unknown parameter $\theta$, for which we use maximum a posteriori estimation (MAP). For this, the parameter $\theta$ is modeled as a random variable with a known priori pdf. This method allows to incorporate the prior knowledge of the parameter through the prior pdf. If the prior is properly chosen, one can expect a better estimate of $\theta$. We model $\mu$, $\sigma$ and $\eta$ as independent Gaussian random variables.

$$\begin{aligned} f(\theta) = p(\mu, \sigma, \eta) &= f(\mu)f(\sigma)f(\eta) \\ &= (2\pi)^{-0.5}|V_\theta|^{-0.5} \\ &\quad \times \exp(-0.5(\theta - m_\theta)^t V_\theta^{-1}(\theta - m_\theta) \end{aligned} \qquad (16)$$

where $m_\theta$ is the vector of means of $\mu$, $\sigma$ and $\eta$ and $V_\theta$ is a diagonal matrix whose entries are variances of the above random variables.

The prior probability parameters $m_\theta$ and $V_\theta$ are chosen using the prior knowledge of the HRF. It is observed that when a stimulus of small duration (unit impulse) is applied, the HRF follows after some delay and attains peak after 2–6 seconds of application of the stimulus. Also, HRF lasts for a duration between 7 to 12 seconds. It is also observed that the amplitude of the response $\eta$ is around 3–5% of the signal intensity. Accordingly, the priors for $\mu$, $\sigma$ and $\eta$ can be chosen as [5]:

$$\begin{aligned} p(\mu) &\sim N(m_\mu, \sigma_\mu) = N(6, 1.732) \\ p(\sigma) &\sim N(m_\sigma, \sigma_\sigma) = N(2, 2.24) \\ p(\eta) &\sim N(m_\eta, \sigma_\eta) = N(4, 2.24) \end{aligned}$$

where, $m_\mu$, $m_\sigma$ and $m_\eta$ are means, and $\sigma_\mu$, $\sigma_\sigma$ and $\sigma_\eta$ are standard deviations of $\mu$, $\sigma$ and $\eta$, respectively. Therefore, the prior probability $p(\theta)$ can be specified as:

$$\begin{aligned} p(\theta) &\sim N(m_\theta, V_\theta), \quad where \\ m_\theta &= [m_\mu, m_\sigma, m_\eta]^t = [6, 2, 4]^t \\ V_\theta &= \alpha diag(\sigma_\mu^2, \sigma_\sigma^2, \sigma_\eta^2) = diag(3, 5, 5) \end{aligned}$$

The unknown parameters to be estimated are parameters of HRF $\theta$ and the drift component $\beta$. The origin of drift in fMRI time-series is not known. But it is observed that it is a low frequency signal. In this work, we estimate the drift in the wavelet domain using the information that it is a low frequency signal. Therefore, its wavelet coefficients at lower scales (high frequencies) should be negligible and can be assumed to be zero. Hence the wavelet coefficients for the drift component can be written as:

$$\begin{aligned} \beta_w = \big[ &ay_1^J, dy_1^J, dy_1^{J-1}, \ldots, dy_{2^{-J}N}^{J-1}, \\ &\ldots, dy_1^{Jo}, \ldots, dy_{2^{-Jo}N}^{Jo}, 0, 0 \ldots 0 \big]' \end{aligned} \qquad (17)$$

where, $Jo$ is the lowest scale up to which the drift component is significant. $a\beta_k^j$ and $d\beta_k^j$ are, respectively, approximate and detail coefficients of $\beta_\mathbf{w}$. We observed from null fMRI data that the drift component is significant only at first two higher scales. Therefore we assume $Jo = J - 2$. We use the following iterative algorithm to estimate the unknown parameters:

1. Initialize the algorithm assuming a linear trend. Estimate its parameters using the data in the rest blocks of the design paradigm. Subtract this component from the data. Let $\mathbf{y_{wd}}$ are the wavelet coefficients of the detrended voxel time-series.
2. Find a least square estimate of $\mathbf{h}$

$$\hat{\mathbf{h}}_{ls} = \left(\mathbf{X}_w^t \mathbf{X}_w\right)^{-1} \mathbf{X}_w^t \mathbf{y}_{wd} \qquad (18)$$

3. Remove the signal component from the time-series

$$\tilde{\mathbf{y}}_\mathbf{w} = \mathbf{y_w} - \mathbf{X_w}\hat{\mathbf{h}}_{\mathbf{ls}} \qquad (19)$$

4. Estimate the drift component $\hat{\beta}_\mathbf{w}$ by equating the wavelet coefficients to zero from scale $Jo - 1$ to 1.
5. Now, use the estimated drift in the wavelet domain and find the MAP estimate of $\theta$ as:

$$\begin{aligned} \theta_{MAP} &= arg\ max_\theta\ p(\mathbf{y}_w|\mathbf{h})p(\theta) \\ &= arg\ min_\theta\ (\mathbf{y}_w - \mathbf{X}_w\mathbf{h}(\theta) - \hat{\beta}_w)^t(\Lambda)^{-1} \\ &\quad \times (\mathbf{y}_w - \mathbf{X}_w\mathbf{h}(\theta) - \hat{\beta}_w) + \theta^t V_\theta^{-1}\theta \quad (20) \end{aligned}$$

where, the prior probability $p(\theta) \sim N(\mathbf{m}_\theta, \mathbf{V}_\theta)$ is defined in the previous section. Let $\hat{\mathbf{h}}_{MAP} = \mathbf{h}(\theta_{MAP})$.

6. Repeat the steps (3)–(4) by replacing $\hat{\mathbf{h}}_{\mathbf{ls}}$ by $\hat{\mathbf{h}}_{MAP}$ until convergence.

This algorithm converges in 2 to 3 iterations. The above algorithm is applied at each voxel time-series.

### 4.2. *Smooth FIR filter model for hemodynamic response function*

In this section, we model the HRF by a smooth FIR filter using the approach of Ref. 1. In Ref. 1, the noise space is assumed to be spanned by second order polynomial functions. In this work, we model fMRI noise component as a fBm process.

The observed time-series model for a voxel with the wavelet transformed drift component $\beta_{\mathbf{w}}$ estimated and removed is given by:

$$\mathbf{y}_w = \mathbf{X}_w \mathbf{h} + \mathbf{e}_w \qquad (21)$$

where, $\mathbf{h}$ is modeled by a smooth FIR filter. The pdf of $\mathbf{y}_w$ given $\mathbf{h}$ is

$$p(\mathbf{y}_w|\mathbf{h}) \sim N(\mathbf{X}_w \mathbf{h}, \mathbf{\Lambda}) \qquad (22)$$

where, $\Lambda$ is a diagonal matrix given by 14.

In modeling HRF by a FIR filter, no specific shape for HRF is assumed. The task is to estimate filter coefficients for each voxel time-series. Since HRF lasts for about 12–20 seconds, the number of filter coefficients $(K)$ are chosen as $K = 20/TR$. Since the number of coefficients to be estimated is large, this estimation problem is ill-posed. In Ref. 1, the problem is regularized by imposing a smoothing constraint on HRF. The HRF is assumed to be a smooth function of time. This smoothness information is translated into the constraint that the norm of second derivative of the HRF $||h(t)''||$, should be small, and then a corresponding pdf is specified as in Ref. 1. The prior pdf of $\mathbf{h}$ takes the following form

$$p(\mathbf{h}|\epsilon) \propto \epsilon^{(K-1)}$$

$$\times exp\left(-\frac{\epsilon^2}{2TR^2}\sum_{k=0}^{K}(h_{k+1} - 2h_k + h_{k-1})^2\right)$$

$$p(\mathbf{h}|\epsilon) \propto \epsilon^{(K-1)}exp\left(-\frac{\epsilon^2}{2}\mathbf{h}^t\mathbf{M}_p\mathbf{h}\right) \qquad (23)$$

where, $\mathbf{M}_p$ is a concentration matrix given by:

$$\mathbf{M_p} = \frac{1}{(TR)^4}\begin{pmatrix} 5 & -4 & 1 & 0 & \ldots & \ldots & \ldots & 0 & 0 \\ -4 & 6 & -4 & 1 & 0 & \ldots & \ldots & 0 & 0 \\ 1 & -4 & 6 & -4 & 1 & 0 & \ldots & \ldots & 0 \\ 0 & 1 & -4 & 6 & -4 & 1 & 0 & \ldots & \vdots \\ 0 & \ddots & \ddots & \ddots & \ddots & \ddots & \ddots & \ddots & \\ \vdots & & 0 & 1 & -4 & 6 & -4 & 1 & 0 \\ \vdots & \ldots & & 0 & 1 & -4 & 6 & -4 & 1 \\ & & & & 0 & 1 & -4 & 6 & -4 \\ 0 & & \ldots & \ldots & 0 & 0 & 1 & -4 & 5 \end{pmatrix}. \qquad (24)$$

The relative weight of this prior to data is controlled by the hyper parameter $\epsilon$. Also the starting and final values of HRF are assumed to be zero. (i.e., $h(0) = h(K) = 0$). Hence, only $(K-1)$ filter parameters are to be estimated.

Jeffrey's prior is assumed for $\epsilon$ as given below,[1] since there is no prior knowledge of $\epsilon$.

$$p(\epsilon) = (\epsilon)^{-1} \qquad (25)$$

Using Bayes rule, the joint posterior pdf for $\mathbf{h}$ and $\epsilon$ can be written as:

$$p(\mathbf{h}, \epsilon|\mathbf{y_w}) \propto p(\mathbf{y_w}|\mathbf{h}, \epsilon)p(\mathbf{h}|\epsilon)p(\epsilon) \qquad (26)$$

Therefore, the required marginal posterior pdf for $\mathbf{h}$ is given by:

$$p(\mathbf{h}|\mathbf{y_w}) = \int p(\mathbf{h}, \epsilon|\mathbf{y_w})d\epsilon \qquad (27)$$

There is no closed form solution to this marginal pdf and numerical optimization is required to find the MAP estimate of $\mathbf{h}$. To overcome this problem, $\epsilon$ is first estimated by MAP and then the a posteriori pdf for $\mathbf{h}$ is approximated as:

$$p(\mathbf{h}|\mathbf{y_w}) \approx p(\mathbf{h}|\mathbf{y_w}, \epsilon = \hat{\epsilon}) \qquad (28)$$

where $\hat{\epsilon}$, the MAP estimate of $\epsilon$ is given by:

$$\hat{\epsilon} = arg_\epsilon \ max \ p(\epsilon|\mathbf{y_w}) \tag{29}$$

The marginal posterior probability for $\epsilon$ is easy to evaluate and is given by:

$$p(\epsilon|\mathbf{y_w}) \propto (det(M(\epsilon))^{-1/2}\epsilon^{\frac{(K-1)}{2}}$$
$$\times exp\big(-1/2\big(\mathbf{y_w}^t\Lambda^{-1}\mathbf{y_w}$$
$$-\hat{\mu_B}^t M(\epsilon)\hat{\mu_B}\big)$$
$$where, \ M(\epsilon) = X_w^t\Lambda^{-1}X_w + \epsilon^2 M_p$$
$$and, \ \hat{\mu_B} = M(\epsilon)^{-1}(X_w^t\Lambda^{-1}\mathbf{y_w}) \tag{30}$$

Now, the task is to estimate the HRF $\mathbf{h}$. The fMRI model

$$\mathbf{y_w} = X_w\mathbf{h} + \mathbf{e_w} \tag{31}$$

is a classical Bayesian linear model.[13] The posterior probability of $\mathbf{h}$ given $\mathbf{y_w}$ and an estimate of $\epsilon$ can be easily evaluated using the standard results.[13] Since the process $\mathbf{e_w}$ and the prior pdf of $\mathbf{h}$ are Gaussian, the posterior pdf of $\mathbf{h}$ will also be Gaussian with posterior mean and covariance given by

$$E(\mathbf{h}|\mathbf{y}_w,\hat{\epsilon}) = \big(\mathbf{X}_w^t\mathbf{\Lambda}^{-1}\mathbf{X}_w + \hat{\epsilon}^2\mathbf{M}_p\big)^{-1}\mathbf{X}_w^t\mathbf{\Lambda}^{-1}\mathbf{y}_w \tag{32}$$

$$C_{\frac{h}{y}} = \big(\mathbf{X}_w^t\mathbf{\Lambda}^{-1}X_w + \hat{\epsilon}^2\mathbf{M}_p\big)^{-1} \tag{33}$$

The conditional expectation of $\mathbf{h}$, $E(\mathbf{h}|\mathbf{y},\hat{\epsilon})$ is its minimum mean square estimator (MMSE). The factor $\alpha = \hat{\epsilon}^2$ determines the relative weight of the prior information. We get a maximum likelihood estimate (MLE) for $\alpha = 0$.

The algorithm given in the previous section can be used to estimate the HRF $\mathbf{h}$ and the drift component $\beta$ by replacing $\hat{\mathbf{h}}_{MAP}$ in that algorithm by the MMSE estimate of $\mathbf{h}$ given by (32).

### 4.3. *Estimation of covariance matrix*

We need the covariance matrix $\Lambda$ for the above algorithm. The diagonal elements of $\Lambda$ are nothing but variance of wavelet coefficients at each scale and are related to the Hurst component $\sigma_j^2 = \sigma_b^2 2^{-(2H+1)j}$, where $j$ is the scale and $\sigma_b$ is an unknown parameter. Therefore variance of wavelet coefficients can be estimated by estimating $H$ and $\sigma_b$ using a large number of algorithms in the literature.[7] But these algorithms are found to be not reliable for $H > 0$.[14] Another way of estimating the variance at each scale is to use simple sample variance estimator.[15] fMRI

time-series are typically of length 128 or less. The length of wavelet coefficients at scale $j$ will be $N/2^j$. Hence, sample variance estimator will be unreliable due to small data lengths. In Ref. 15, it is shown that variance estimators will be more reliable using the undecimated wavelet transforms (UWT) compared to the conventional non-redundant discrete wavelet transforms (DWT). In UWT, the length of wavelet coefficients will be $N$ irrespective of the scale. In this work, we use DWT for estimating the unknown parameters $\theta$ and $\beta$ and UWT for estimating the variances at each scale.

## 5. Test Bed

We test the above algorithms first on a synthetic fMRI noise and then on a real fMRI data obtained when the subject is at rest performing no cognitive or physical task. We call such data as "null" data. Below, we briefly discuss the method used for generating the synthetic fBM noise.

### 5.1. *Generation of synthetic data*

Time-series with $1/f$-like power spectrum (also called as $1/f$ process) can be generated using several methods. Wavelet transforms which decorrelate these class of signals can be used to synthesize these signals. We use a wavelet based method suggested in Ref. 9. The variance of detailed coefficients $d_j$, at each scale $j$ is related to the Hurst component (H) as

$$var(d_j) = \sigma_b^2(2^j)^{2H+1} \tag{34}$$

This relation is used to generate $1/f$ process. At each scale $j$, Gaussian noise with above variance is generated. The required time-series is generated by taking inverse wavelet transform. We use orthogonal daubechies-4 wavelet with four levels of decomposition. The parameter $\sigma_b^2$ is decided by the required signal to noise ratio (SNR). The SNR is calculated as:

$$SNR = 10 \ log_{10} E_s/\sigma_w^2 \tag{35}$$

where, $E_s$ is the BOLD signal energy and $\sigma_w^2$ is the noise power. We fix the value of $H$ as 0.4. $E_s$ is estimated as $\mathbf{h'h}$, where $\mathbf{h}$ is HRF, modeled as a Gaussian function with typical parameters $\theta = [6, 2, 4]$. Since orthogonal transformation preserves

energy, the noise power $\sigma_w^2$ is the sum of variances in each scale $j$.

$$\sigma_w^2 = \sigma^2 \sum_{j=1}^{J} (2^j)^{2H+1} \qquad (36)$$

where, $J$ is the maximum scale allowed. The parameter $\sigma_b^2$ can be calculated for a given SNR. Using the above method, We generate synthetic fMR images with size $16 \times 16$, where each voxel is a time-series of length 64. The fMR data is generated at SNRs = 5, 0, $-5$ and $-10$ dB. A quadratic trend is added to this data to simulate low frequency trends in the fMRI data. We assume sampling rate $(TR)$ of 1 second and data at $TR = 2$ and $TR = 3$ are generated by subsampling the data generated for the sampling period of 1 second.

## 5.2. *Null data*

The null data is acquired at National Institute of Medical Health and NeuroSciences, Bangalore, India, using a 1.5 Tesla Siemens machine. The scanning sequence was a single-shot gradient-echo ($T2^*$ weighted) with 66 ms echo time and 90 degrees RF flip angle with a matrix size of $128 \times 128$. The data is acquired when the subject is at rest. The sampling time interval between two consecutive acquisitions is 1 second $(TR = 1)$.

We assume that the subject is at rest from 1 to 10 seconds, followed by activation from 10 to 20 seconds and then again rest. Thus the experimental paradigm is modeled as a boxcar function with ones from 10 to 20 seconds and zeros at the other times. The BOLD signal is modeled as a convolution of this boxcar function with HRF as shown in the Fig. 1. In the parametric method, we model HRF by a Gaussian function. To study the influence of this model on other HRF shapes, we use Poisson and Gamma functions to simulate HRF in addition to Gaussian function and model them all by Gaussian function. The convolution of these HRF functions with boxcar function is added to both synthetic and null fMRI data. In the nonparametric
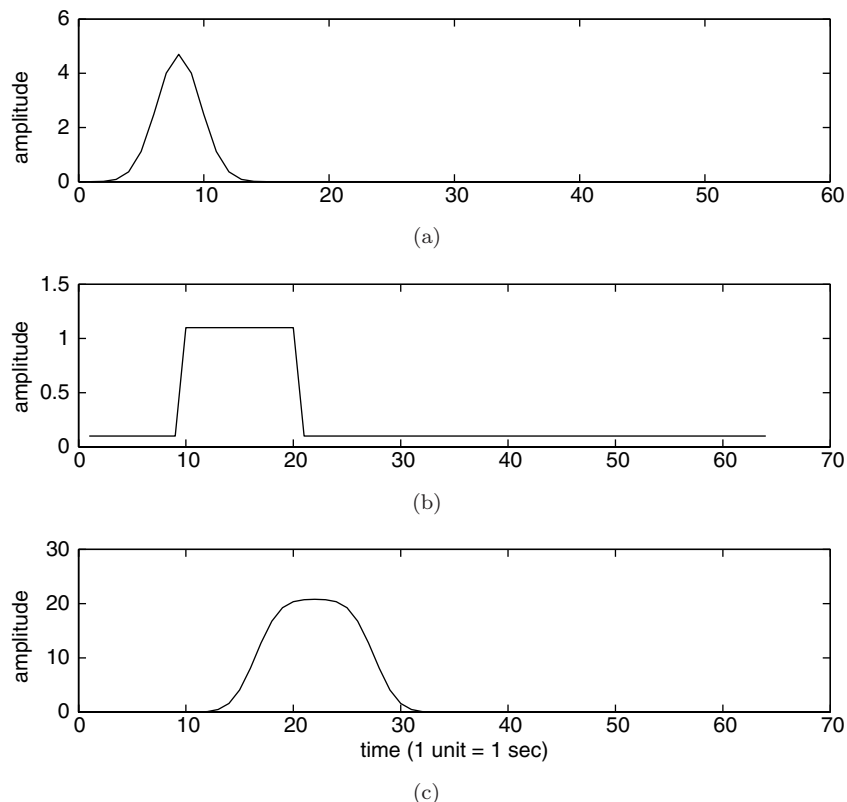


Fig. 1. Linear model for blood oxygen level dependent (BOLD) signal (a) HR function (b) Input activation profile or design paradigm (c) BOLD response: convolution of HR and input activation.

case, we test whether the FIR filter model for HRF is able to model parametric HRF models like Gaussian, Poisson and Gamma functions. We also study the influence of sampling rate on $HRF$ estimation. The performances of these two methods are characterised by the performance indices defined in the next section.

## 6. Results and Discussion

We compare the performance of the above two algorithms on synthetic and real (null) fMRI data using the following performance indices.

### 6.1. *Performance measures*

We use the following performance indices to quantify the performance of the proposed methods. We use Gaussian model to fit other parametric functions like Poisson and Gamma.

1. Time to peak $t_p$ is an important parameter of HRF. It characterises the delay in response to a given task. This parameter can be used to find the relative time of activation of various regions. In our case, since Gaussian function is used to model all the types of HRFs, the mean $\mu$ of the estimated Gaussian function represents the time to peak. The percentage error in the estimation of time to peak is defined as:

$$\delta t_p = \frac{|\hat{\mu} - \mu|}{\mu} \times 100 \qquad (37)$$

where, $\hat{\mu}$ is the estimated time to peak and $\mu$ is the actual time to peak. Mean of the Gaussian function and parameter of the Poisson model, respectively, characterize the time to peak. In the Gamma model, the ratio of Gamma function parameters characterizes the time to peak.

2. The amplitude of the response $\eta$ to a given stimulus is also an important parameter which characterizes the strength of the response at each voxel. The percentage error in the estimation of this parameter is defined as:

$$\delta \eta = \frac{|\hat{\eta} - \eta|}{\eta} \times 100 \qquad (38)$$

where, $\hat{\eta}$ is the estimated amplitude and $\eta$ is the actual amplitude of HRF.

3. The overall error in the estimation of the HRF is characterized by the sample mean square error (MSE) which is defined as:

$$MSE = (\hat{\mathbf{h}} - \mathbf{h})^t (\hat{\mathbf{h}} - \mathbf{h})/K \qquad (39)$$

where, $\hat{\mathbf{h}}$ and $\mathbf{h}$ are, respectively, the estimated and actual HRF and $K$ is the length of the response.

4. The sample correlation ($\rho$) between the estimated ($\hat{\mathbf{h}}$) and actual HRF ($\mathbf{h}$) measures the match between them. The range of $\rho$ is from 0 to 1, where 1 corresponds to a perfect match.

In the smooth FIR model, we calculate the time to peak ($t_p$ or group delay) of HRF using

$$t_p = \frac{\sum_{k=0}^{K} k h(k)}{\sum_{k=0}^{K} h(k)} \qquad (40)$$

The amplitude of HRF is estimated as the peak of the estimated HRF.

### 6.2. *Synthetic data*

Tables 1 and 2 summarize the performances of the parametric and FIR filter methods for different SNRs, TRs and HRF functions. The parametric method results in 15–20% error each in the estimation of time to peak and amplitude, respectively, at $TR = 1$ for all HRF models and SNRs. The performance is robust for decreasing SNR. The sample correlation is more than 0.8. In the case of FIR model, the estimation error is about 3–8% and 7–18% in the estimation of time to peak and amplitude, respectively, at $TR = 1$ for all HRF models and SNRs. The sample correlation is more than 0.9. Hence, FIR filter performance is better than that of Gaussian model for $TR = 1$. However, at $TR = 2$, the performance of FIR filter model is poorer than the parametric method. Also, performance decreases with the decrease in SNR. At $TR = 3$, the estimation of HRF becomes very unreliable.

Table 1. Performance comparison of parametric method at different SNRs and TRs. Poisson, Gamma and Gaussian simulated hemodynamic response functions are modeled by a Gaussian Function. fMRI noise is modeled by fractional Brownian motion. poi: Poisson, gam: Gamma, gau: Gaussian, $\delta t_p$: percent error in time to peak, $\delta\eta$: percent error in amplitude, $MSE$: Mean square error in HRF estimation and $\rho$: sample correlation between actual and estimated HRFs.

| SNR (dB) | TR (sec) | $\delta t_p$ | | | $\delta\eta$ | | | $MSE$ | | | $\rho$ | | |
|---|---|---|---|---|---|---|---|---|---|---|---|---|---|
| | | poi | gam | gau | poi | gam | gau | poi | gam | gau | poi | gam | gau |
| 5 | 1 | 19 | 20 | 16.4 | 12 | 11 | 13.2 | 1.95 | 1.8 | 1.12 | 0.85 | 0.83 | 0.84 |
| 5 | 2 | 26 | 28 | 24 | 22 | 24.7 | 24.2 | 2.3 | 2.5 | 1.96 | 0.6 | 0.5 | 0.62 |
| 5 | 3 | 26 | 27 | 28 | 28 | 27.4 | 29 | 2.76 | 3 | 2.98 | 0.55 | 0.48 | 0.46 |
| 0 | 1 | 18.6 | 20.3 | 16.5 | 17 | 16 | 18.58 | 1.96 | 1.88 | 1.31 | 0.81 | 0.82 | 0.81 |
| 0 | 2 | 20 | 21 | 18.2 | 25 | 24 | 25.35 | 2.1 | 2.11 | 2.4 | 0.63 | 0.68 | 0.61 |
| 0 | 3 | 26 | 27 | 29 | 23 | 22.1 | 23.13 | 3.35 | 3.1 | 2.9 | 0.53 | 0.49 | 0.48 |
| −5 | 1 | 18 | 20 | 16.6 | 21 | 20 | 19 | 2 | 1.96 | 1.4 | 0.82 | 0.81 | 0.81 |
| −5 | 2 | 23 | 25 | 27 | 24 | 27 | 26 | 2.73 | 2.88 | 2.9 | 0.62 | 0.64 | 0.65 |
| −5 | 3 | 31 | 32 | 33 | 30 | 33 | 34 | 3.4 | 3.5 | 3.2 | 0.46 | 0.45 | 0.43 |
| −10 | 1 | 17 | 18 | 15 | 18 | 16.4 | 15 | 1.76 | 1.73 | 1.4 | 0.81 | 0.79 | 0.78 |
| −10 | 2 | 24 | 23 | 24 | 27 | 28 | 24 | 2.75 | 2.9 | 2.82 | 0.55 | 0.58 | 0.59 |
| −10 | 3 | 33.7 | 34 | 32 | 32 | 33.2 | 34 | 3.7 | 3.5 | 3.4 | 0.47 | 0.46 | 0.43 |

Table 2. Performance comparison of nonparametric method at different SNRs and TRs. Poisson,Gamma and Gaussian simulated hemodynamic response functions are modeled by a smooth FIR filter. fMRI noise is modeled by fractional Brownian motion. poi: Poisson, gam: Gamma, gau: Gaussian.

| SNR (dB) | TR (sec) | $\delta t_p$ | | | $\delta\eta$ | | | $MSE$ | | | $\rho$ | | |
|---|---|---|---|---|---|---|---|---|---|---|---|---|---|
| | | poi | gam | gau | poi | gam | gau | poi | gam | gau | poi | gam | gau |
| 5 | 1 | 3 | 2.7 | 2.3 | 7.2 | 12 | 14 | 0.38 | 0.35 | 0.43 | 0.97 | 0.96 | 0.95 |
| 5 | 2 | 26 | 27 | 23.4 | 26 | 29 | 36 | 2.9 | 2.77 | 2.84 | 0.51 | 0.52 | 0.54 |
| 5 | 3 | 33 | 31 | 27 | 29 | 31 | 32 | 3.4 | 3.8 | 3.7 | 0.44 | 0.42 | 0.49 |
| 0 | 1 | 4.1 | 4.6 | 5 | 7.4 | 15.5 | 15 | 0.8 | 0.8 | 0.84 | 0.93 | 0.93 | 0.9 |
| 0 | 2 | 28 | 29 | 25.4 | 28 | 30 | 37 | 3.1 | 3.2 | 3.3 | 0.53 | 0.52 | 0.51 |
| 0 | 3 | 31 | 37 | 42 | 34 | 35 | 31 | 4.2 | 4.3 | 4.4 | 0.38 | 0.39 | 0.41 |
| −5 | 1 | 5.2 | 5.5 | 5.3 | 7.7 | 17 | 18 | 1.5 | 1.6 | 1.72 | 0.87 | 0.85 | 0.82 |
| −5 | 2 | 32 | 33 | 39 | 27 | 29 | 30 | 3.7 | 3.6 | 3.5 | 0.46 | 0.45 | 0.47 |
| −5 | 3 | 41 | 49 | 66 | 34 | 37 | 35 | 6.5 | 6.4 | 6.2 | 0.3 | 0.35 | 0.34 |
| −10 | 1 | 6.2 | 7.5 | 8 | 12 | 17.2 | 17.1 | 3.28 | 3.38 | 3.4 | 0.8 | 0.74 | 0.73 |
| −10 | 2 | — | — | — | — | — | — | — | — | — | — | — | — |
| −10 | 3 | — | — | — | — | — | — | — | — | — | — | — | — |

### 6.3. *Null Data*

Now, we apply both parametric and nonparametric methods on the null fMRI data. Figures 2 and 3, respectively, show the performance of parametric and FIR modeling methods at TR = 1, 2 and 3 seconds. At TR = 1 sec, the errors in the estimation accuracies of time to peak and amplitude are about

14–18% and 12–14%, respectively, for all the three simulated HRFs for the parametric method. FIR filter method is able to estimate these parameters with accuracies of about 3% and 10%, respectively. The sample correlation $\rho$ between the estimated and the actual HRFs is about 0.82 for parametric case and is about 0.9 for nonparametric model. Hence at low
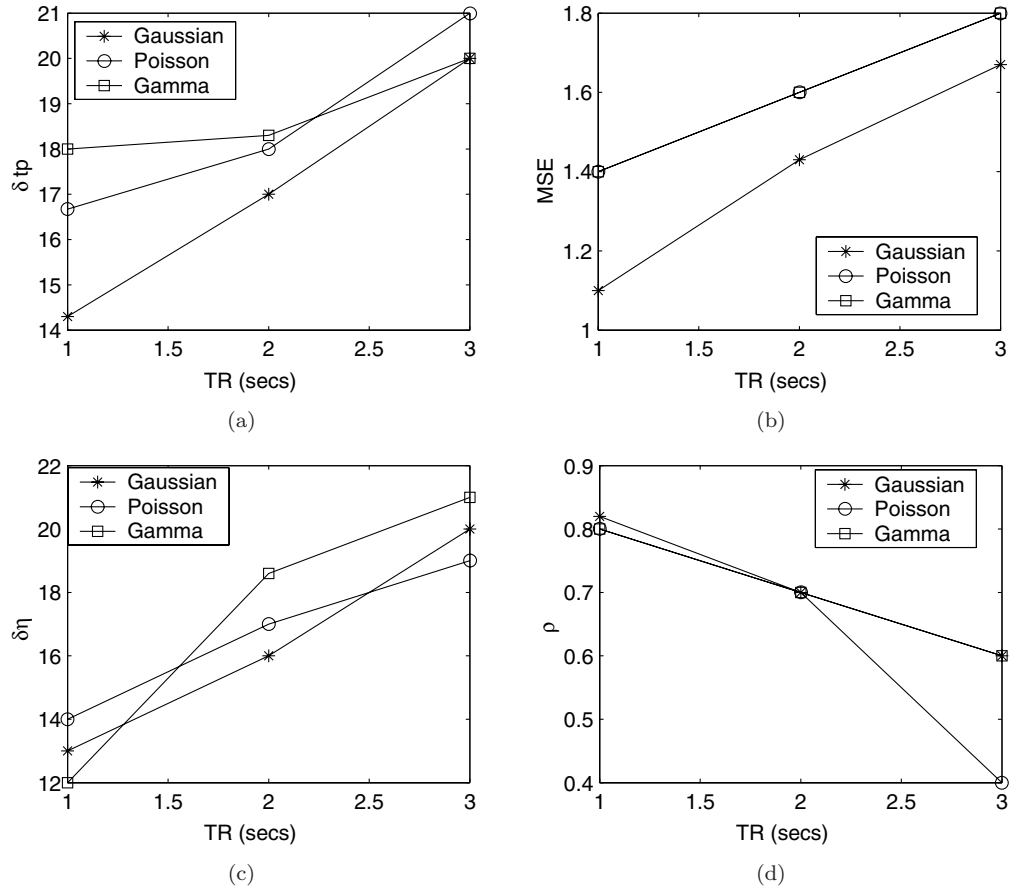
Fig. 2.   Performance measures for parametric modeling of HRF as a function of TR. fMRI noise is modeled by fractional Brownian motion. (a) Percentage error in the estimation of time to peak ($\delta t_p \times 100$) (b) MSE (c) Percentage error in the estimation of amplitude of HRF ($\delta\eta \times 100$) (d) Correlation between estimated and actual HRF ($\rho$).
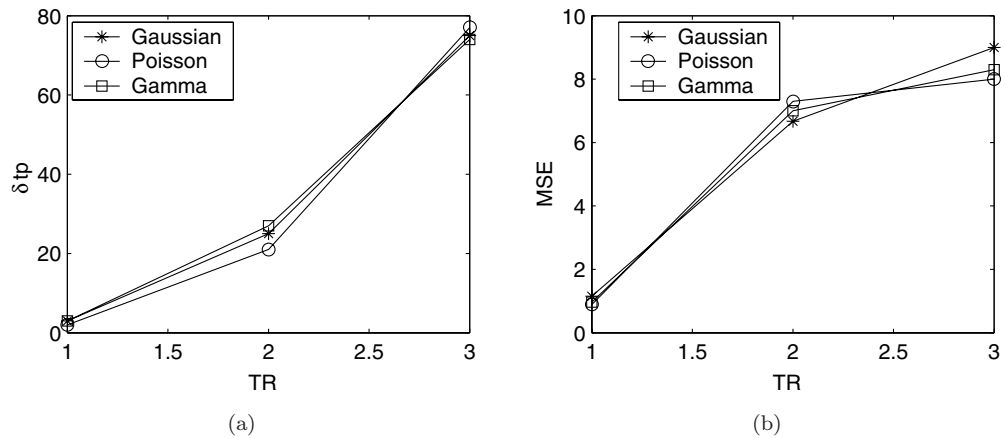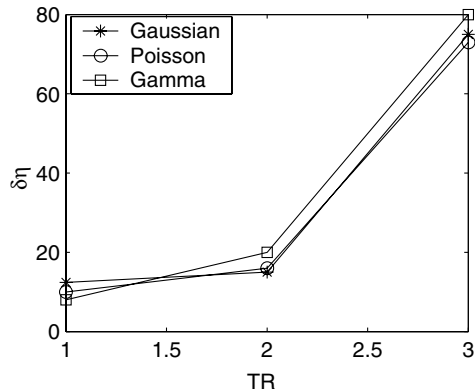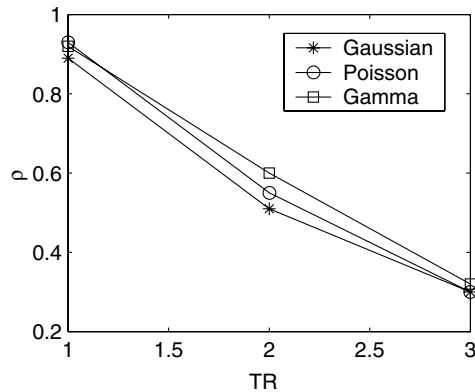


Fig. 3.   Performance measures for nonparametric modeling of HRF as a function of TR. fMRI noise is modeled by fractional Brownian motion. (a) Percentage error in the estimation of time to peak ($\delta t_p \times 100$) (b) MSE (c) Percentage error in the estimation of amplitude of HRF ($\delta\eta \times 100$) (d) Correlation between estimated and actual HRF ($\rho$).

Fig. 3. (*Continued*)

TRs, both parametric and FIR filter models are able to recover HRFs with good accuracy. But at higher TRs, the ability of FIR filter to model HRFs diminishes as compared to parametric model which is also evident from the simulated data. At TR = 2 sec, the errors in the estimation accuracies of time to peak and amplitude are about 18% and 17%, respectively, for all the three simulated HRFs for the parametric method, whereas FIR filter method is able to estimate these parameters with accuracies of only 25% and 17%, respectively. The sample correlation for parametric case is about 0.7 and for FIR case, it is only 0.5. Hence parametric model performs better at higher TRs.

### 6.4. *Overall comparison*

We also compare the performance of fBm noise model for the smooth FIR filter method with the method of Ref. 1. In Ref. 1, the drift component is modeled by polynomial bases and the noise component by white Gaussian noise. The model is given by

$$\mathbf{y} = \mathbf{X}\mathbf{h} + \mathbf{P}\lambda + \mathbf{e} \tag{41}$$

where $\mathbf{y}$ is the observed time-series, $\mathbf{X}$ is the convolution matrix, the columns of $\mathbf{P}$ represent polynomial bases of degree 2, $\lambda$ are the unknown coordinates of component along the polynomial bases and $\mathbf{e}$ is white Gaussian noise with an unknown variance. The HRF $\mathbf{h}$ is modeled by a smooth FIR filter. We apply this method on both synthetic and null fMRI data. Table 3 summarizes the performance of this method on the synthetic data at different SNRs and

TRs. By comparing this Table with Table 2, the following conclusions can be drawn. The performance using fBm model is superior to the polynomial model of Ref. 1. For example, at $SNR = 0$ dB and $TR = 1$ second, the estimation errors in time to peak $\delta t_p$ is about 4.5% for fBm model for all the simulated HRF parametric models (Gaussian, Poisson and Gamma). On the other hand, polynomial noise model gives about 10% error. The mean square error values of 0.8 using fBm model, is less compared to the value of 1.2 achieved by the polynomial model. At this $SNR$ and $TR$, the value of the correlation coefficient $\rho$, 0.9, obtained by fBm model is superior to 0.8, achieved by the polynomial model. Performances of these two models degrade with the decrease in $SNR$ and increase in $TR$. The degradation in performance is more severe in the polynomial model. Table 4 summarizes the results obtained for SNR = 0 dB and $TR = 1$ second for fBm and polynomial models.

In the case of null data, for $TR = 1$ second, the fBm model is able to estimate the time to peak with an accuracy of 3%. Polynomial model gives an accuracy of about 7%. At this $TR$, MSE using fBm model is about 0.9, which is less than the value of 1.1 achieved by the polynomial model. The values of fidelity index $\rho$, obtained by fBm model, is about 0.92, which is superior to the value of 0.85 achieved by the polynomial model. Figure 4 shows the performance of the model involving polynomial bases. For both the models, HRF estimation becomes unreliable with increase in $TR$. From this, we can conclude that the fBm noise model is superior to the adhoc polynomial bases, for modeling the baseline drifts and fMR

Table 3. Performance comparison of nonparametric method at different SNRs and TRs. Poisson, Gamma and Gaussian simulated hemodynamic response functions are modeled by a smooth FIR filter. Trends are modeled by polynomial bases of degree 2. poi: Poisson, gam: Gamma, gau: Gaussian, $\delta t_p$: percent error in time to peak, $\delta\eta$: percent error in amplitude, $MSE$: Mean square error in HRF estimation and $\rho$: sample correlation between actual and estimated HRFs.

| SNR (dB) | TR (sec) | $\delta t_p$ | | | $\delta\eta$ | | | $MSE$ | | | $\rho$ | | |
|---|---|---|---|---|---|---|---|---|---|---|---|---|---|
| | | poi | gam | gau | poi | gam | gau | poi | gam | gau | poi | gam | gau |
| 5 | 1 | 8.54 | 8.61 | 11.3 | 8.5 | 12.7 | 21 | 0.87 | 1 | 1.3 | 0.91 | 0.88 | 0.81 |
| 5 | 2 | 24 | 25 | 24 | 25 | 29.3 | 29 | 2.97 | 2.4 | 2.73 | 0.51 | 0.52 | 0.56 |
| 5 | 3 | 26 | 27 | 30 | 31 | 32 | 31 | 3.67 | 3.44 | 3.7 | 0.38 | 0.39 | 0.4 |
| 0 | 1 | 8.7 | 9.2 | 12 | 6.4 | 9.4 | 19 | 1 | 1.2 | 1.5 | 0.89 | 0.85 | 0.8 |
| 0 | 2 | 20 | 21 | 25 | 27 | 28.2 | 27.3 | 2.3 | 2.6 | 3 | 0.51 | 0.55 | 0.53 |
| 0 | 3 | 25 | 28 | 31 | 32 | 31.6 | 34 | 3.8 | 4 | 4.7 | 0.4 | 0.39 | 0.38 |
| −5 | 1 | 10 | 11.4 | 11 | 14 | 12 | 11 | 2 | 2.2 | 2.4 | 0.8 | 0.8 | 0.7 |
| −5 | 2 | 20 | 17 | 21 | 29 | 28 | 27 | 4.5 | 4 | 4.6 | 0.47 | 0.44 | 0.49 |
| −5 | 3 | 31 | 35 | 33 | 34 | 33 | 31 | 13 | 9 | 7 | 0.31 | 0.34 | 0.4 |
| −10 | 1 | 12 | 8 | 24 | 14 | 11 | 12 | 5 | 5 | 5.6 | 0.7 | 0.65 | 0.55 |
| −10 | 2 | — | — | — | — | — | — | — | — | — | — | — | — |
| −10 | 3 | — | — | — | — | — | — | — | — | — | — | — | — |

Table 4. Comparison of fMRI models on synthetic data at $SNR = 0\,\mathrm{dB}$ and $TR = 1\,\mathrm{sec}$. HRF is modeled by Smooth FIR filter.

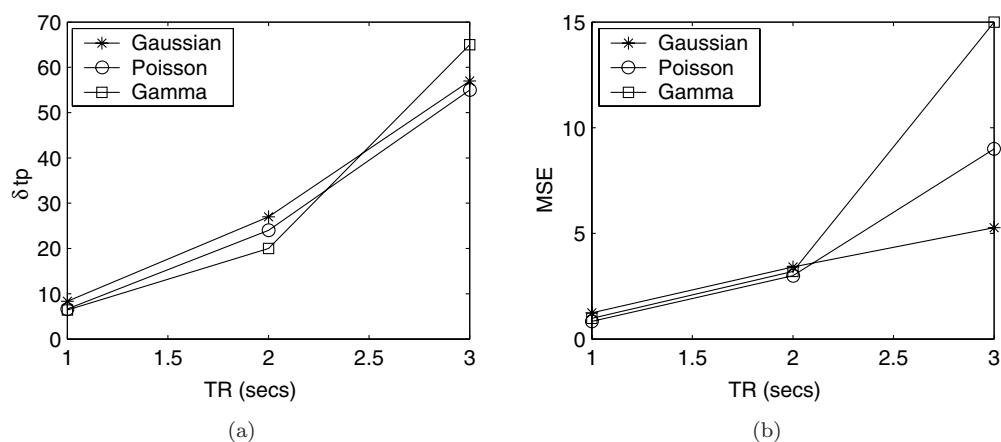| Methods | $\delta t_p$ | | | $\delta\eta$ | | | $MSE$ | | | $\rho$ | | |
|---|---|---|---|---|---|---|---|---|---|---|---|---|
| | poi | gam | gau | poi | gam | gau | poi | gam | gau | poi | gam | gau |
| fBm | 4.1 | 4.6 | 5 | 7.4 | 15.5 | 15 | 0.8 | 0.8 | 0.84 | 0.93 | 0.93 | 0.9 |
| Poly. Bases | 8.7 | 9.2 | 12 | 6.4 | 9.4 | 19 | 1 | 1.2 | 1.5 | 0.89 | 0.85 | 0.8 |



Fig. 4. Performance measures for nonparametric modeling of HRF as a function of TR. Trends are modeled by polynomial bases of degree 2. (a) Percentage error in the estimation of time to peak ($\delta t_p \times 100$) (b) MSE (c) Percentage error in the estimation of amplitude of HRF ($\delta\eta \times 100$) (d) Correlation between estimated and actual HRF ($\rho$).
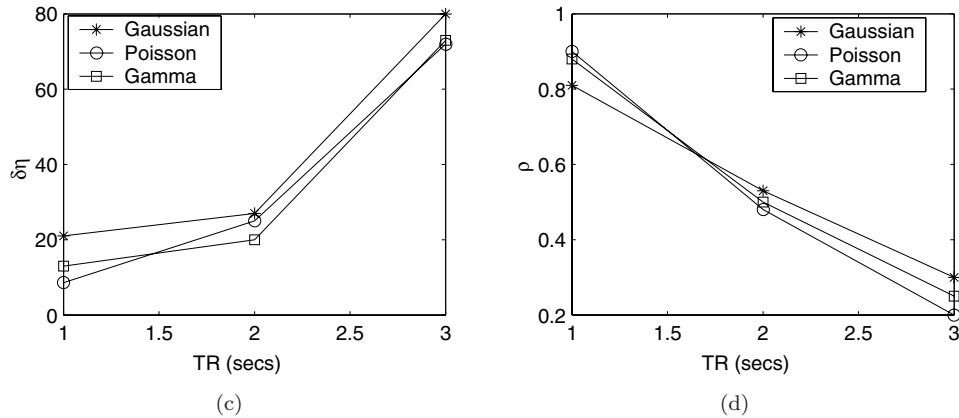
Fig. 4. (*Continued*)

Table 5. Comparison of fMRI models on Null data at $TR = 1$ sec. HRF is modeled by Smooth FIR filter.

| Methods | $\delta t_p$ | | | $\delta\eta$ | | | $MSE$ | | | $\rho$ | | |
|---|---|---|---|---|---|---|---|---|---|---|---|---|
| | poi | gam | gau | poi | gam | gau | poi | gam | gau | poi | gam | gau |
| fBm | 2 | 3 | 3 | 10 | 8 | 12.4 | 0.9 | 0.97 | 1.15 | 0.93 | 0.92 | 0.9 |
| Poly. Bases | 6.64 | 6.4 | 8.35 | 8.6 | 13 | 21 | 0.9 | 1.0 | 1.24 | 0.9 | 0.88 | 0.81 |

noise. Table 5 summarizes the results obtained at $TR = 1$ second on the null data for both the models.

## 7. Conclusions

We proposed wavelet based methods for the estimation of hemodynamic response function for both Gaussian and FIR filter models. The fMRI noise which exibhits $1/f$-like spectrum is modeled as a fractional Brownian Motion. The probability models are built on the assumption that wavelet transforms with sufficient number of vanishing moments decorrelate a fBm process. The baseline drifts are also estimated along with HRF. We also compared fBm model with the exisisting method of [1] which uses polynomial bases for modeling baseline drifts and smooth FIR filter model for HRF. fBm model using smooth FIR filter model for HRF are found to be superior to the method of Ref. 1. At lower $TR$s, nonparametric model performs better than the parametric methods.

## References

1. G. Marrelec, H. Benali, P. Ciuliu and J. B. Pioline, Bayesian estimation of the hemodynamic response function in functional MRI, in Bayesian Inference and Maximum Entropy Methods, (ed.) R. Fry (Baltimore, MD): Max Ent Workshops (2001).
2. G. M. Boyton, S. A. Engel, G. H. Glover and D. J. Heeger, Linear systems analysis of functional magnetic resonance imaging in human V1, *J. Neuroscience* (1996) 4207–4221.
3. E. Bullmore, C. Long, J. Suckling, J. Fadili, G. Calvert, F. Zelaya, T. Adrian Carpenter and M. Brammer, Colored noise and computational inference in neurophysiological (fMRI) time series analysis: Resampling methods in time and wavelet domain, *Human Brain Mapping* (2001) 61–78.
4. F. Meyer, Wavelet-based estimation of a semiparametric generalized linear model of fMRI timeseries, *IEEE Trans. Medical Imaging* **22**(3) (2003) 315–322.
5. M. Svensen, F. Kruggel and D. Yves von Cramon, Probabilistic modeling of single-trial fMRI data, *IEEE Trans. Medical Imaging* **19**(1) (2000) 25–35.
6. E. Zarahn, G. K. Aguire and M. D. Esposito, Empirical analyses of BOLD fMRI statistics I. Spatially unsmoothed data collected under

null hypothesis conditions, *NeuroImage* **5** (1997) 179–197.

7. G. W. Wornell, Signal Processing with Fractals: A Wavelet-Based Approach (New Jersey:Printice Hall Inc., 1996).

8. J. Beran, Statistics for Long-Memory Processes (Chapman and Hall, 1994).

9. P. Flandrin, Wavelet analysis and synthesis of fractional Brownian motion, *IEEE. Trans. Inform. Theory* **38**(12) (1992) 910–917.

10. A. H. Tewfik and M. Kim, Correlation structure of the discrete wavelet coefficients of fractional Brownian motion, *IEEE. Trans. Inform. Theory* **40** (1994) 1609–1612.

11. G. W. Wornell, A Karhunen-Loeve like expansion for $1/f$ processes via wavelets, *IEEE. Trans. Inform. Theory* **36** (1998) 859–861.

12. R. W. Dijkerman and R. R. Mazumdar, On the correlation structure of the wavelet coefficients of fractional Brownian motion, *IEEE. Trans. Inform. Theory* **40** (1994) 1609–1612.

13. S. Kay, Fundamentals of Statistical Signal Processing: Estimation Theory (Prentice-Hall, New Jersey, 1995).

14. B. Ninness, Estimation of 1/f Noise, *IEEE Trans. on Inform Theory* **44** (1998) 32–46.

15. D. P. Percival, On estimation of wavelet variance, *Biometrika* **82**(3) 619–631.